X-716-65-401

NASA TM X-55380

# THE ATMOSPHERE EXPLORER-B SOLAR ARRAY (AE-B)

N66-17253

| | |
|---|---|
| N66-17253 (ACCESSION NUMBER) | 1 (THRU) |
| 21 (PAGES) | (CODE) |
| (NASA CR OR TMX OR AD NUMBER) | 03 (CATEGORY) |

FACILITY FORM 602

OCTOBER 1965

GPO PRICE $ ______

CFSTI PRICE(S) $ ______

Hard copy (HC) 1.00

Microfiche (MF) .50

ff 653 July 65

NASA

GODDARD SPACE FLIGHT CENTER
GREENBELT, MARYLAND

X-716-65-401

# THE ATMOSPHERE EXPLORER-B SOLAR ARRAY (AE-B)

by

Edwin Moses

October 1965

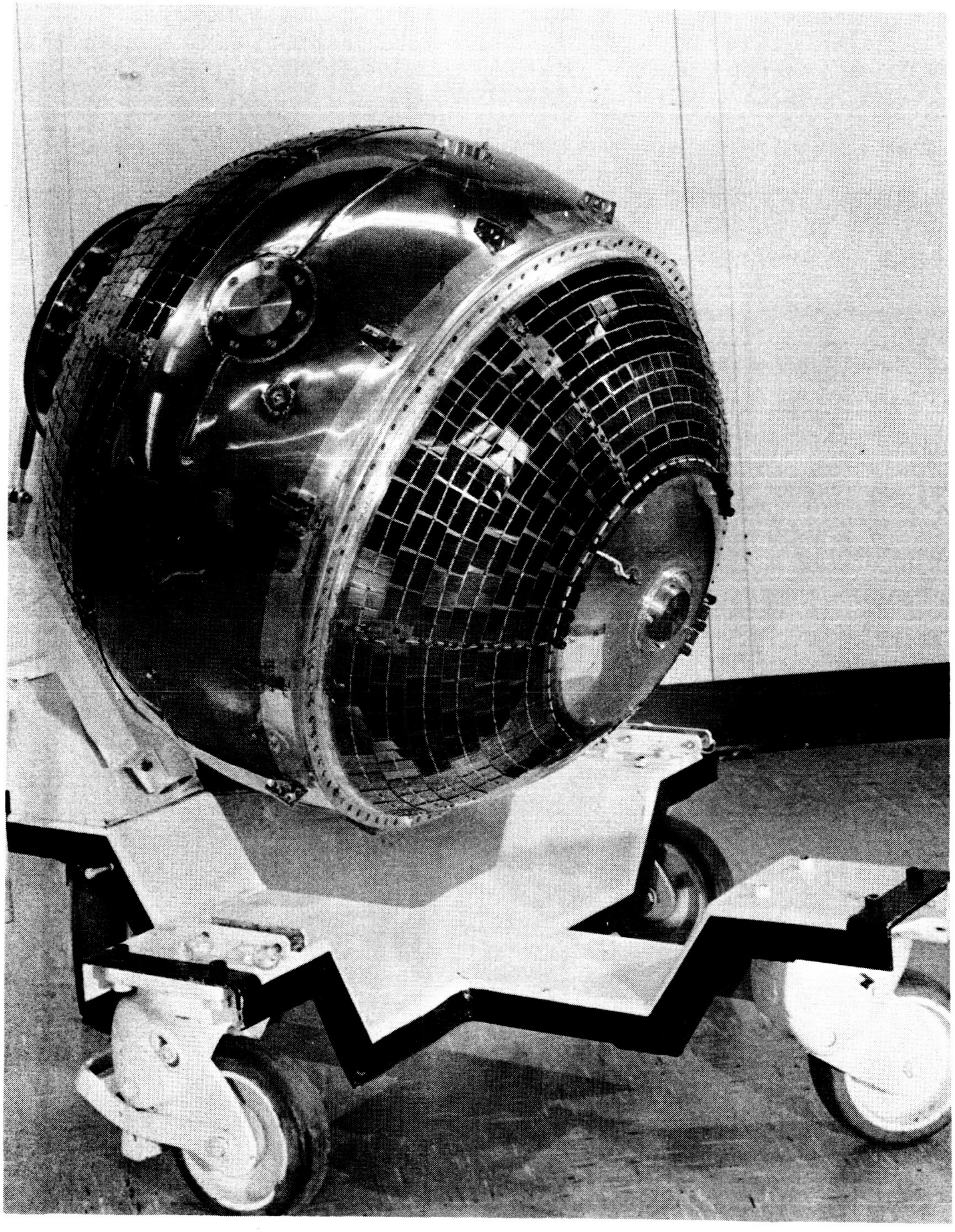

Frontispiece

# THE ATMOSPHERE EXPLORER-B SOLAR ARRAY
# (AE-B)

## INTRODUCTION

In order to extend the life of the AE-B satellite, a solar array has been provided to recharge the spacecraft's silver zinc batteries. Since this type of battery does not possess cyclic lifetime, recharge will be initiated after approximately six months discharge. Each of the satellite's eight battery strings will be alternately switched to the array output which will replace 70% of the energy lost during discharge.

The mission objective of the AE-B solar array is to provide power to recharge the spacecraft's silver zinc batteries after a six-month discharge. This accomplishment will extend the spacecraft lifetime by at least six months.

The power system of the AE-B satellite derives its primary energy from a series of silver zinc battery packs that range from three to twenty volts. The negative source solar array delivers power at 15 volts nominal to the battery charger which reverses the source polarity, converts the voltage level, and selects the particular battery pack to be charged.

The array is composed of 2064 N/P, 2cm x 2cm, gridded solar cells of 1.6 ohm-cm nominal base resistivity. Contacts and grids are sintered titanium-silver. A 6-mil thick fused silica cover glass with an anti-reflective coating on the top and a blue-red filter on the bottom is bonded with Furane Epocast 15-E adhesive to the solar cell. Four cells connected electrically in parallel form the basic building blocks of the array. The module has an air mass zero efficiency of 10% when tested at 0.46 volts at 25°C.

It should be mentioned parenthetically that two factors governed the choice of the 4-cell module configuration; experience on the Nimbus program proved this design to be rugged and reliable, capable of withstanding the cyclic temperature and vibration extremes of that spacecraft, and use of residual cells and modules available from the Nimbus program would result in lower cost.

Forty-three 4-cell modules are connected electrically in series to form an array patch, isolated from other patches by two Motorola 1N3198 diodes wired in parallel. See Figure 1.

Five patches are bonded to the top hemisphere, seven to the bottom. The two negative outputs are joined inside the sphere to form the negative source AE-B solar array. The positive terminal of each patch is grounded to the

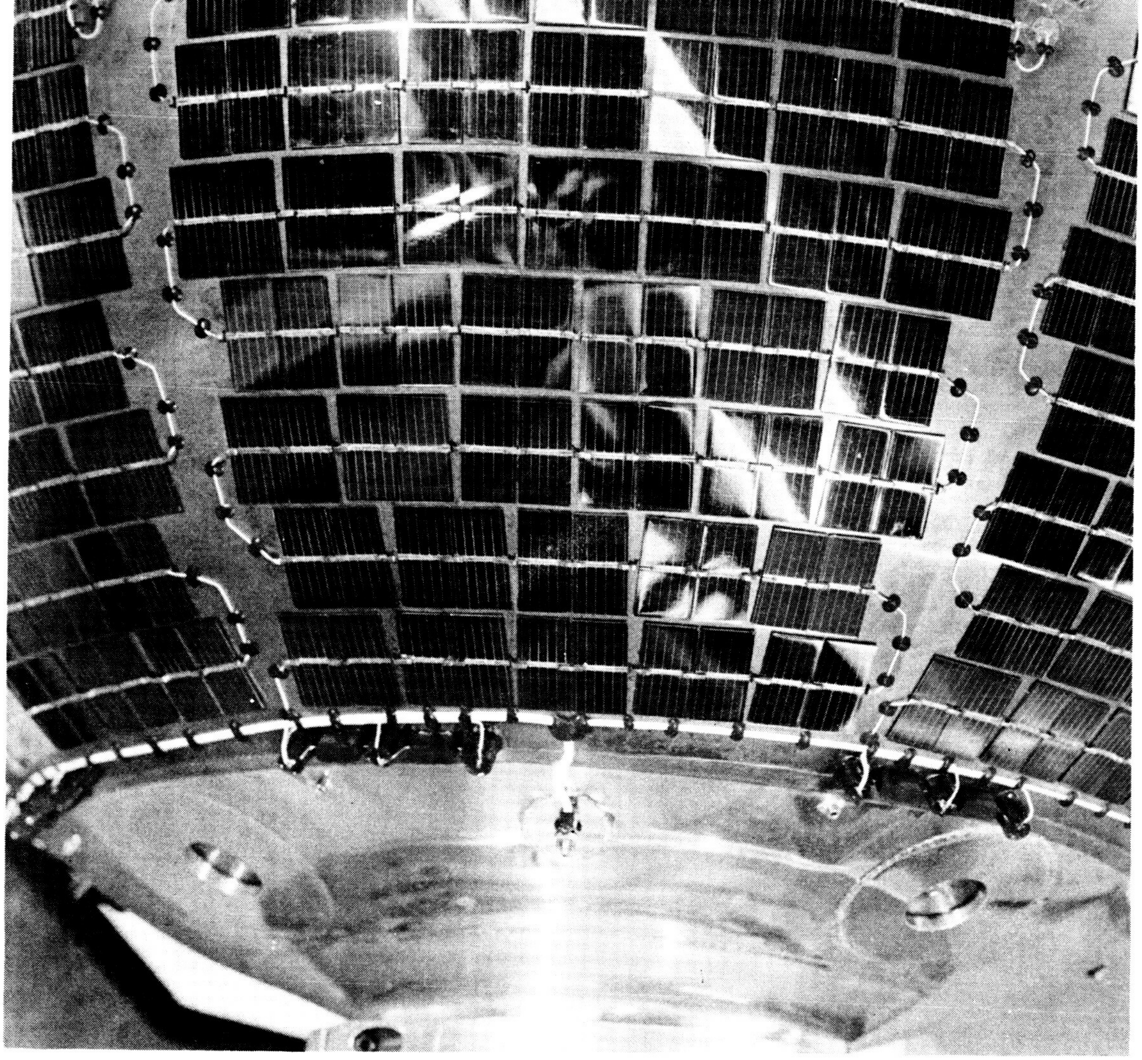

Figure 1

stainless steel sphere to enhance charged particle collection by the experiment's sensors.

Particular care was taken in the preparation of the shell for module bonding to prevent damage to the stainless steel from halide acids and acid halide salts. The shell (see Figure 2) is cleaned with chlorothene and then with a 10-to-1 diluted solution of Hi-Brett metal cleaner. Subsequently, the surface is electrolytically etched with filter paper moistened in a 25% phosphoric acid solution and washed clean with distilled water. The etched area is sprayed with an SMP-62 resin, SMP-63 hardener, and N-butyl alcohol solution to form a dielectric film to electrically insulate the shell from possible contact with the solar cells. The dielectric is cleaned with ethyl alcohol and an RTV silicone rubber primer is applied.

The solar cell modules are attached to weights with double-backed tape, and RTV-60 silicone rubber is applied through a mask on the bottom to form a small cylindrical dot approximately 1 cm in diameter under each cell. After the mask is removed, the module and weight are placed on the shell and held by a locating fixture. The next weight, prepared in the same manner, is positioned adjacent to and butting against its predecessor. A row of modules in a patch is formed before the process repeats on the next row. Therefore, the weights serve not only as pressure to hold the modules through RTV curing, but as spacers between adjacent modules and adjacent rows. Figure 3 shows a bonded patch; the adjacent patch, showing the holding fixture and weights is undergoing a cure cycle.

The isolating diodes are soldered to ceramic standoffs welded to the shell; then diodes and standoffs are encapsulated in RTV-60, leaving the standoff tips available for electrical checkout of the array.

All wiring is bonded to the shell at 1-inch intervals with RTV.

Each patch is covered with a plastic shield to prevent accidental damage to the array before launch. The use of separate shields allows test of one patch while the others remained protected. The plastic will be substituted later by metal to conform to range safety requirements.

Because the array is bonded directly to the satellite substrate, access for electrical checkout was limited. However, the following illumination tests were conducted:

A. Sunlight illumination along the spin axis, top and bottom.

B. Solar simulator illumination of each patch 90° to the spin axis and centered on the patch.

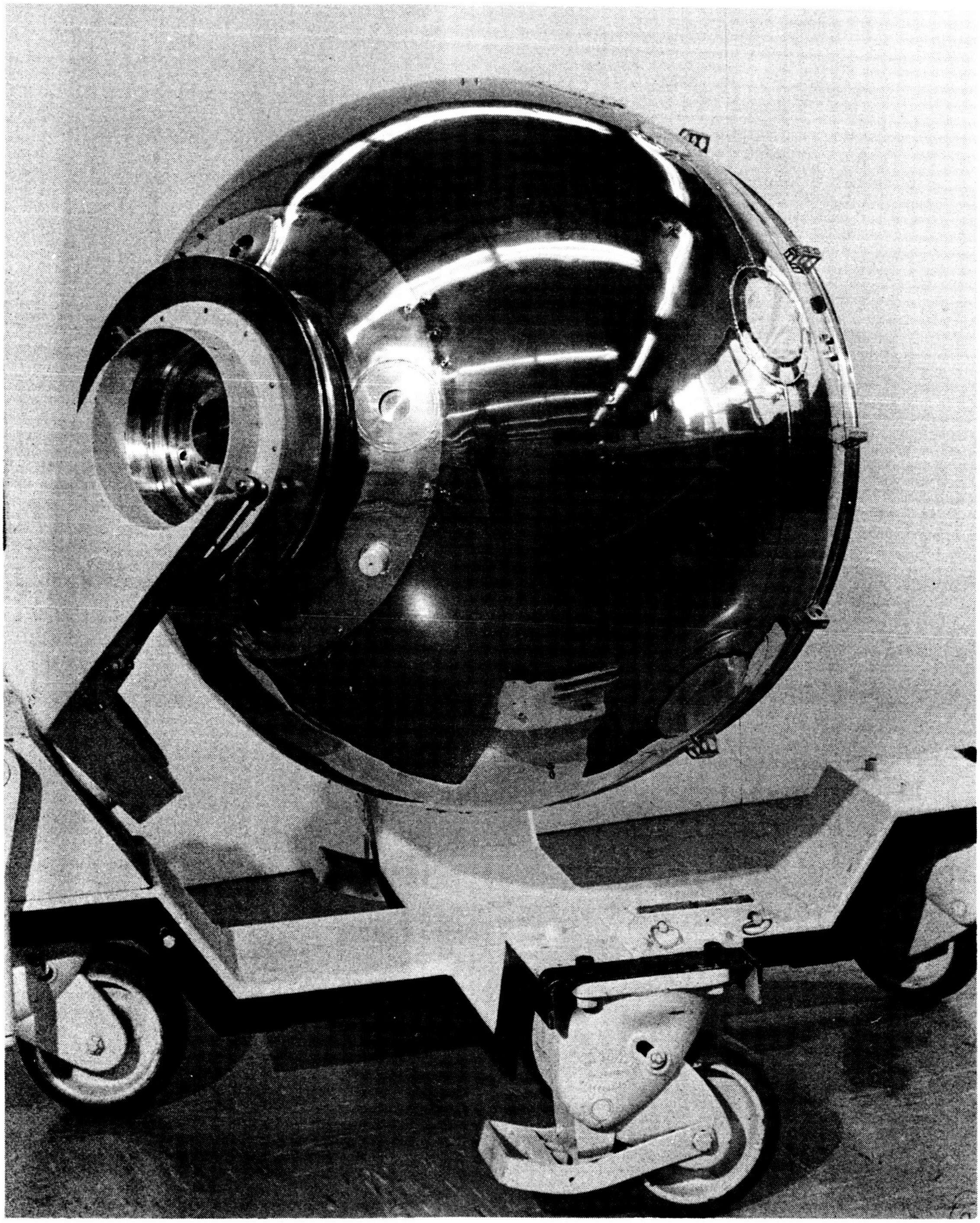

Figure 2

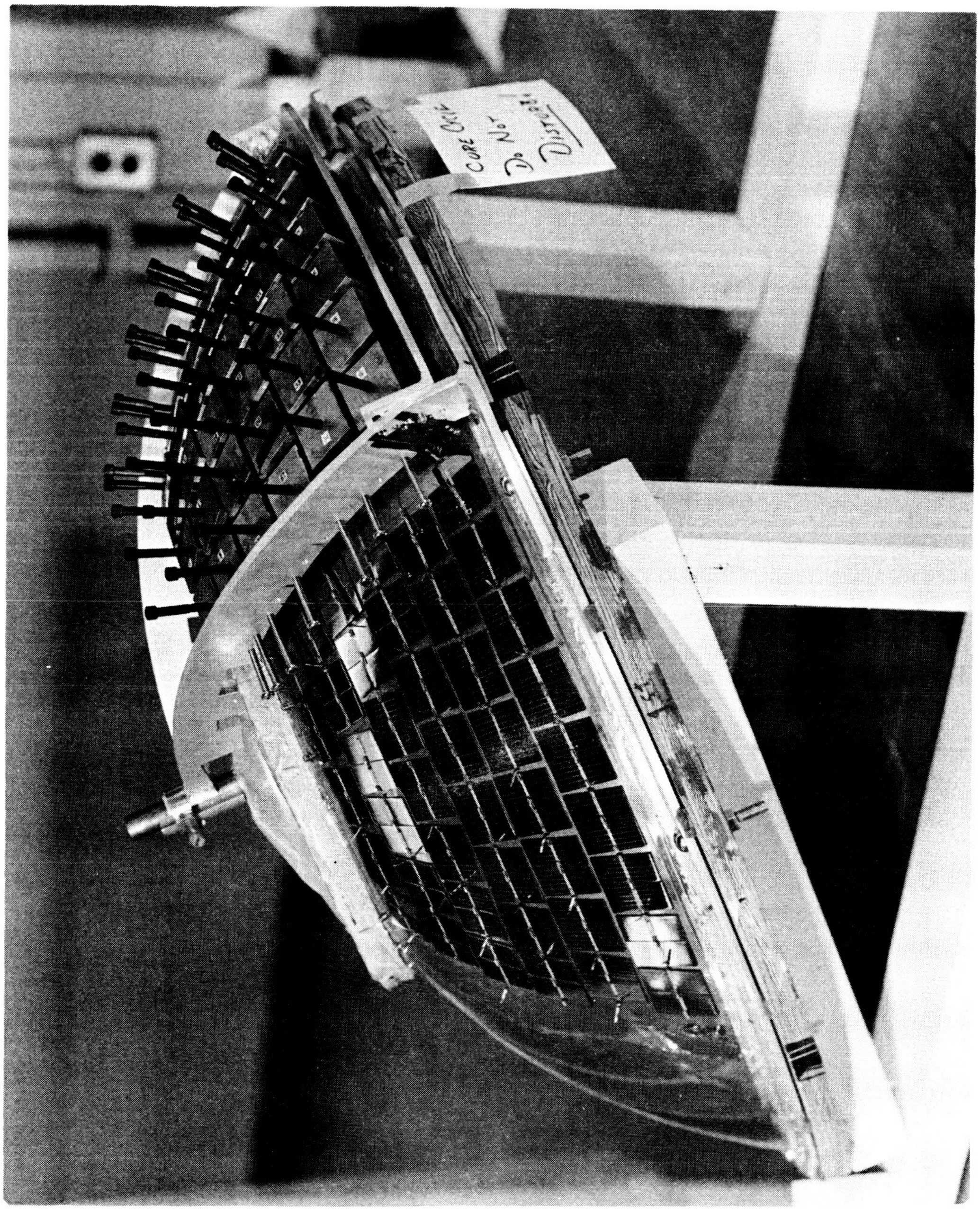

Figure 3

C. Solar simulation of the full array at various aspect and spin angles.

D. Tungsten illumination for pre- and post-environmental test checkout of the array.

To check predictions of power output, the satellite was illuminated along its spin axis in sunlight. With the sphere resting on its dolly, a 3-foot flat black painted cylinder was attached to shield against side radiation. See Figure 4. Attachable to either the top or bottom, this shield halved the output of the array compared to the output without the shield. The shield essentially collimated the light to the limiting rows of modules, those that faced the greatest angle away from the sun, thereby simulating outer space. Thermistors were mounted behind each patch and connected to a recorder. The spin axis was pointed directly toward the sun, the angle being determined by the shadow cast by a pointer mounted on the shield and parallel with the spin axis.

Temperature, collimated and uncollimated standard cell, and pyrheliometer data were recorded simultaneously with the current-voltage characteristic (I-V curve).

Table 1 indicates the results compared with those expected. Considering the low angle of incidence of sunlight on the limiting rows of modules, this correlation is quite acceptable.

In order to further calibrate the array and to gain some measure of space performance, the satellite was tested with a large-area solar simulator. The simulator itself is housed in a 10-foot diameter by 15-foot thermal vacuum chamber. The light array consists of 19 zenon lamps which are reflected by an off-axis parabolic mirror to collimate the light into a 4-foot diameter beam. The light has a collimation angle of two degrees and uniformity of ±10% when tested over the full area with a 1 sq. cm. solar cell detector. Stability is within

Table 1

Sunlight Test Results

| AM = 0 - 25°C - 19.8 volts | | | |
|---|---|---|---|
| Array | Test | Expected | % Error |
| Top | 1.25 amps | 1.32 amps | -5.3% |
| Bottom | 0.740 amps | 0.715 amps | +3.5% |

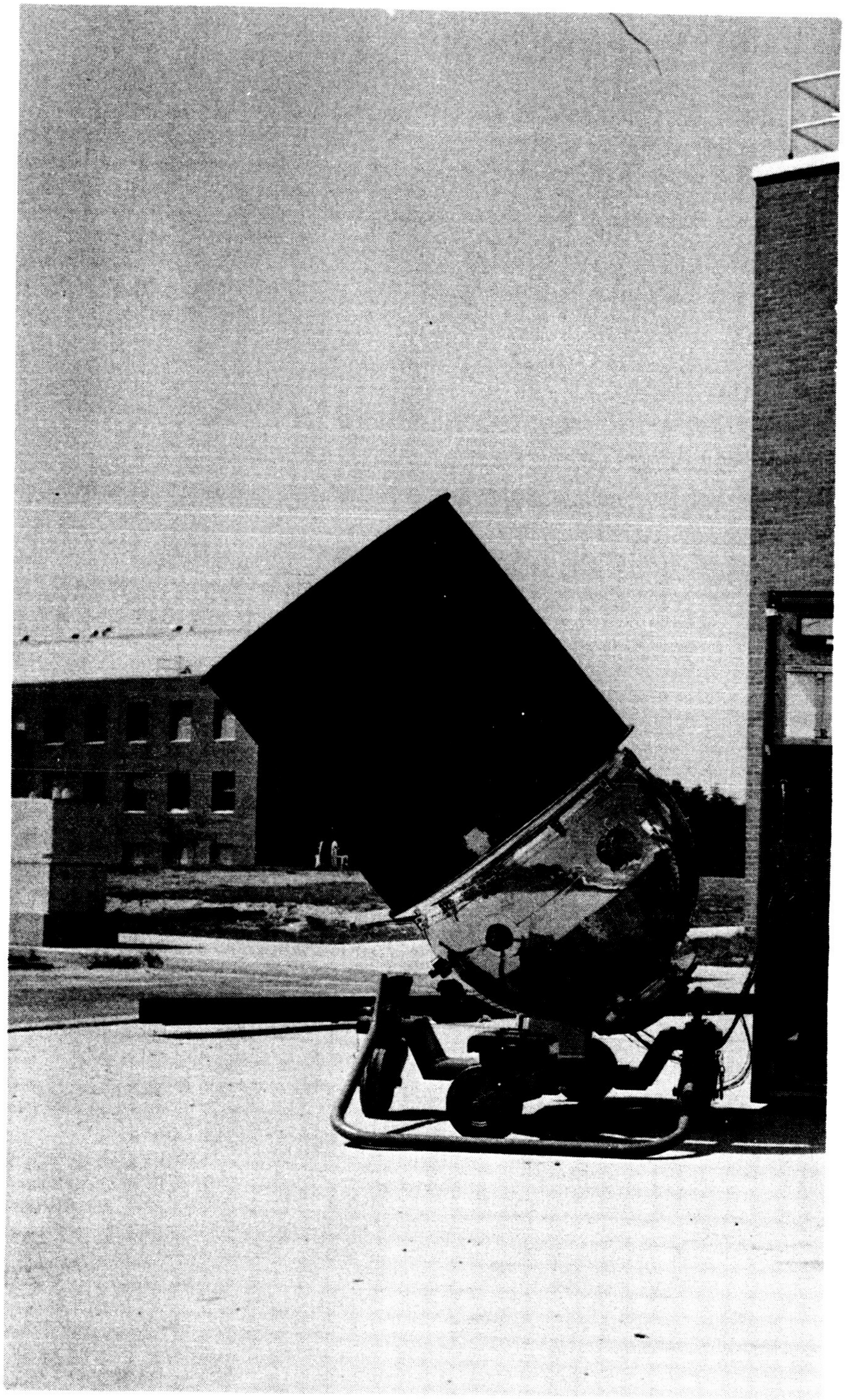

Figure 4

±0.5% over at least a one-week period. Figure 5 compares the light's spectral response with Johnson's air mass zero curve. The high energy content between 0.8 and 1.03 microns indicates why calibration of the light's output by a solar cell standard was necessary. When the light intensity was initially set up with a pyrheliometer, the standard cells read almost a third more than was expected. Consequently, only 12 lights were used.

The satellite was oriented outside of the vacuum chamber directly in the center of the beam (see Figure 6). Each patch was measured separately at a satellite sun angle of 90°; the sphere was then tilted to various sun angles and the total array I-V curve was recorded as spin angles varied from 0° to 180°.

Calibration of the light source intensity was monitored by positioning three solar cell standards normal to the beam in the center of the area to be tested. The cells were lowered out of position while the I-V curve was being recorded.

Table 2 indicates the results of the 90° test after the curves were corrected for uniformity, intensity and temperature variations.

Similar corrections in addition to six months radiation damage were performed on the remaining data, which resulted in the calculated outputs presented

Table 2

Solar Simulator Test Results

| Array | Deviation from Predicted |
|---|---|
| Top #1 | +2.6% |
| 2 | +4.2% |
| 3 | -1.0% |
| 4 | -1.6% |
| 5 | +1.6% |
| Bottom #1 | -2.0% |
| 2 | -4.6% |
| 3 | 0% |
| 4 | -6.0% |
| 5 | -1.5% |
| 6 | -5.5% |
| 7 | -2.0% |

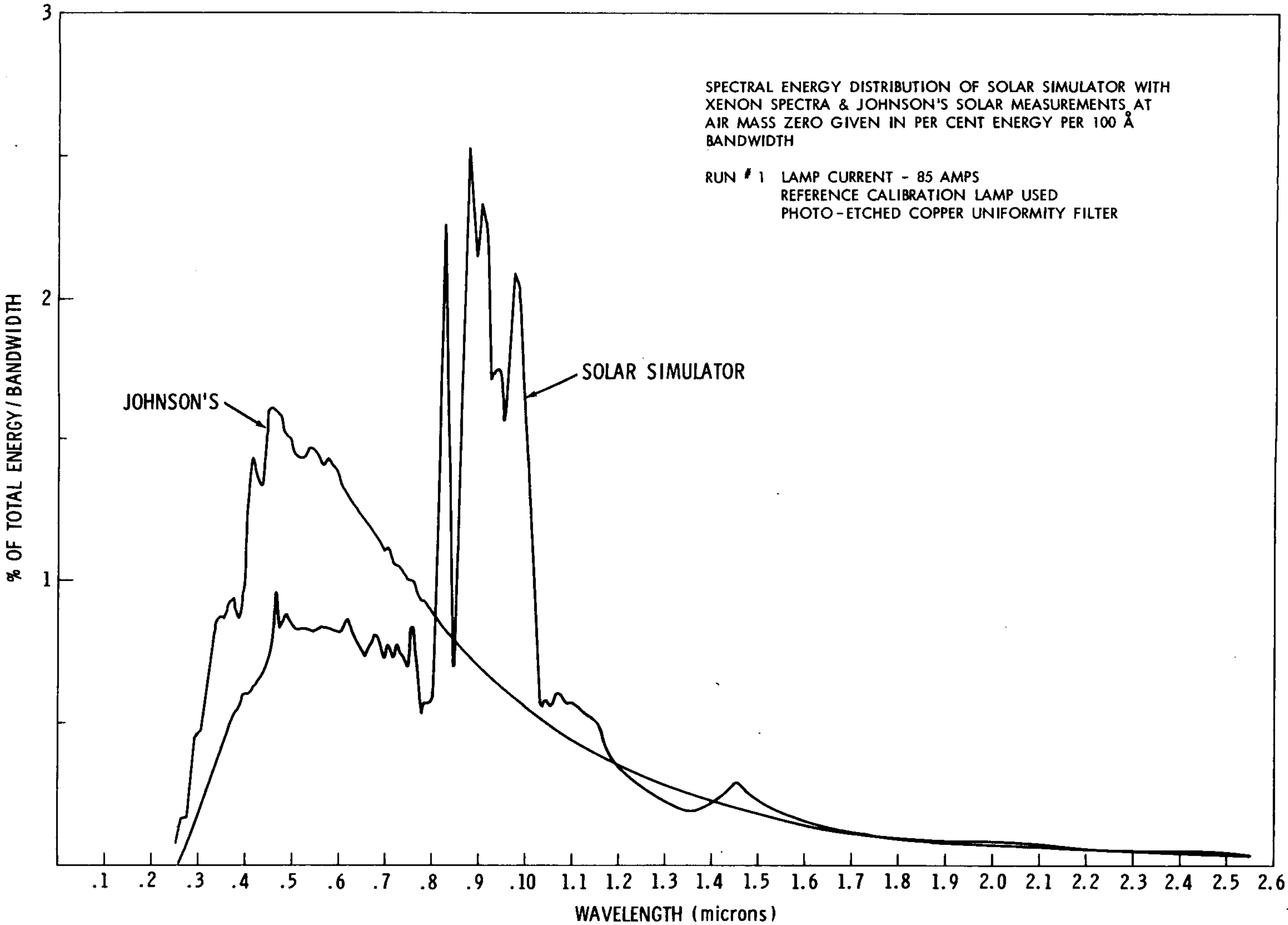

SPECTRAL ENERGY DISTRIBUTION OF SOLAR SIMULATOR WITH XENON SPECTRA & JOHNSON'S SOLAR MEASUREMENTS AT AIR MASS ZERO GIVEN IN PER CENT ENERGY PER 100 Å BANDWIDTH
RUN # 1 LAMP CURRENT - 85 AMPS
REFERENCE CALIBRATION LAMP USED
PHOTO-ETCHED COPPER UNIFORMITY FILTER
JOHNSON'S
SOLAR SIMULATOR
% OF TOTAL ENERGY / BANDWIDTH
3
2
1
.1
.2
.3
.4
.5
.6
.7
.8
.9
.10
1.1
1.2
1.3
1.4
1.5
1.6
1.7
1.8
1.9
2.0
2.1
2.2
2.3
2.4
2.5
2.6
WAVELENGTH (microns)


Figure 5

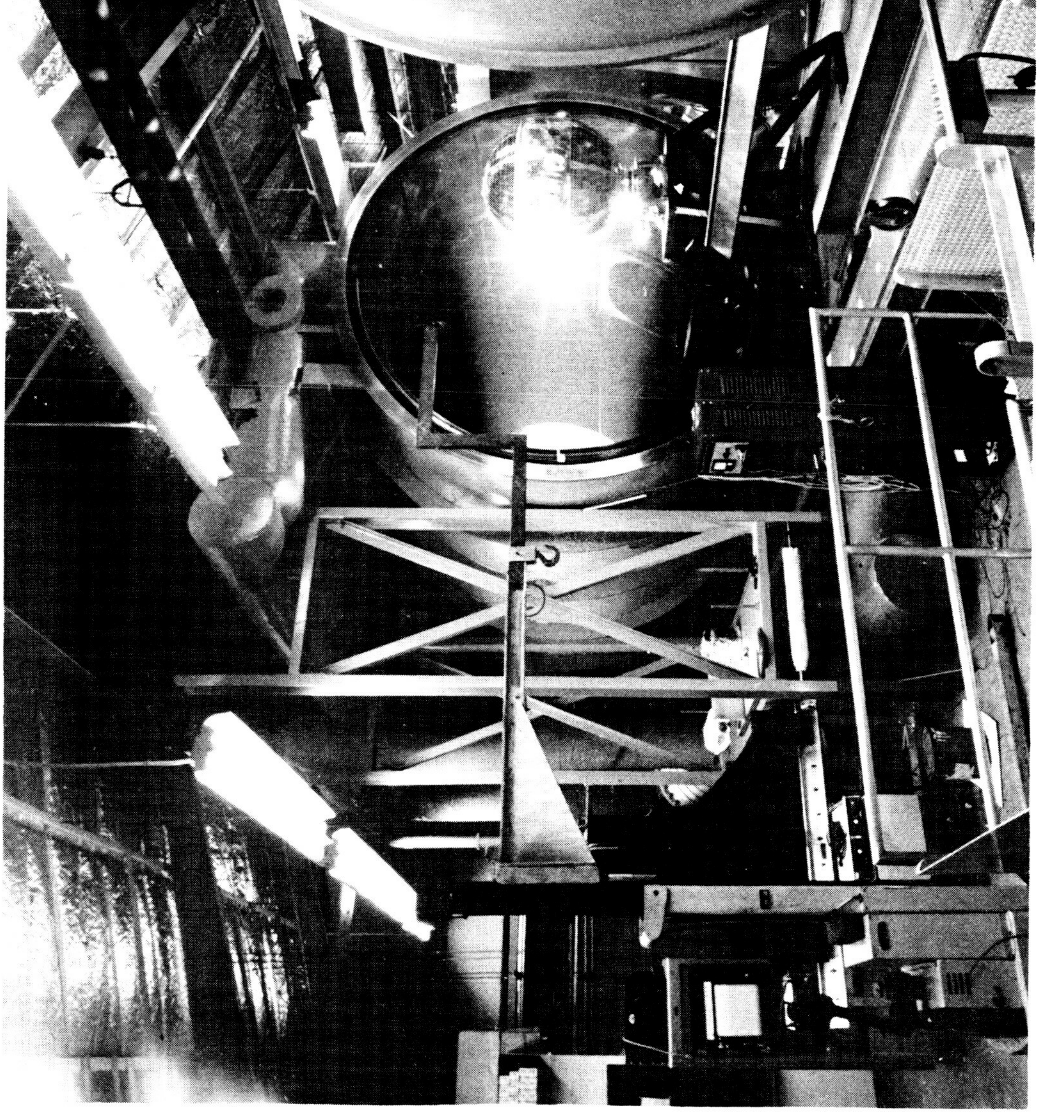

Figure 6

in Table 3. Radiation flux levels predicted for June, 1965 were used for radiation damage purposes. The power was calculated at the intersection of the adjusted I-V curve and the input characteristic of the battery charger.

Table 3

AE-B Solar Array Output

| Solar Aspect Angle | Power after Six Months |
|---|---|
| 30° | 10.8 watts |
| 60° | 8.3 watts |
| 90° | 8.7 watts |
| 120° | 10.4 watts |
| 150° | 8.7 watts |

To assure the integrity of the array through satellite environmental qualification, a special light bank was designed. Since the modules are bonded directly to the satellite substrate, each module lies in a different plane; to detect a failure, the light source should distribute equal illumination to the modules facing at 43 different angles. In practice, this was not achieved; however, sufficient uniformity was provided to detect any failures, particularly high resistance open circuits resulting from cracked cells.

The light source consists of four swivel-mounted 150-watt tungsten bulbs mounted in a rectangular pattern and a fifth bulb wired to a variac. Trial and error methods were used to adjust the position and intensity of the bank. A 2 x 2 cm solar cell was scanned over the surface of a patch to check uniformity. Once satisfactory illumination was achieved, the light bank was hard-mounted to the satellite stand to assure repeatability (see Figure 7. Typical I-V curves are shown in Figure 8, indicating the appearance of high resistance in a patch.

Once a failure is determined within a given patch, each row is tested individually by shorting out the other rows. The failure appears as a poor knee in the case of an open, or as too little open circuit voltage for a given temperature in the case of a short. After the failure is isolated to a particular row, each module is shorted until the knee of the curve increases, or no change in open circuit voltage occurs. In the case of the open, the short across the damaged module removes the limiting generator, allowing full current to flow again; in the case of the shorted module, shorting it again has no effect, as it would on adjacent good modules. Figure 9 shows typical curves of a high resistance open.

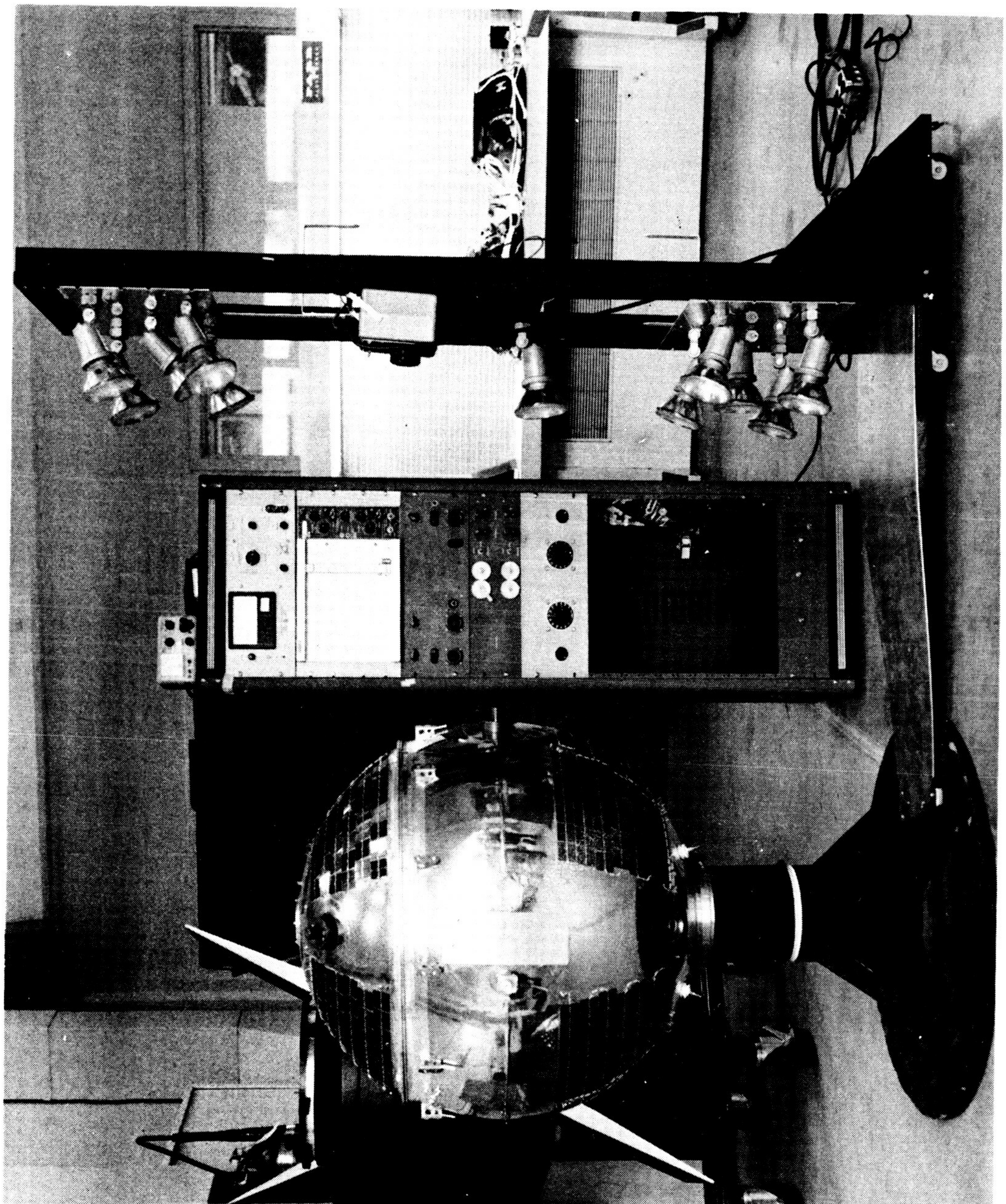

Figure 7

TYPICAL I-V CHARACTERISTICS LOCATING A HIGH RESISTANCE MODULE

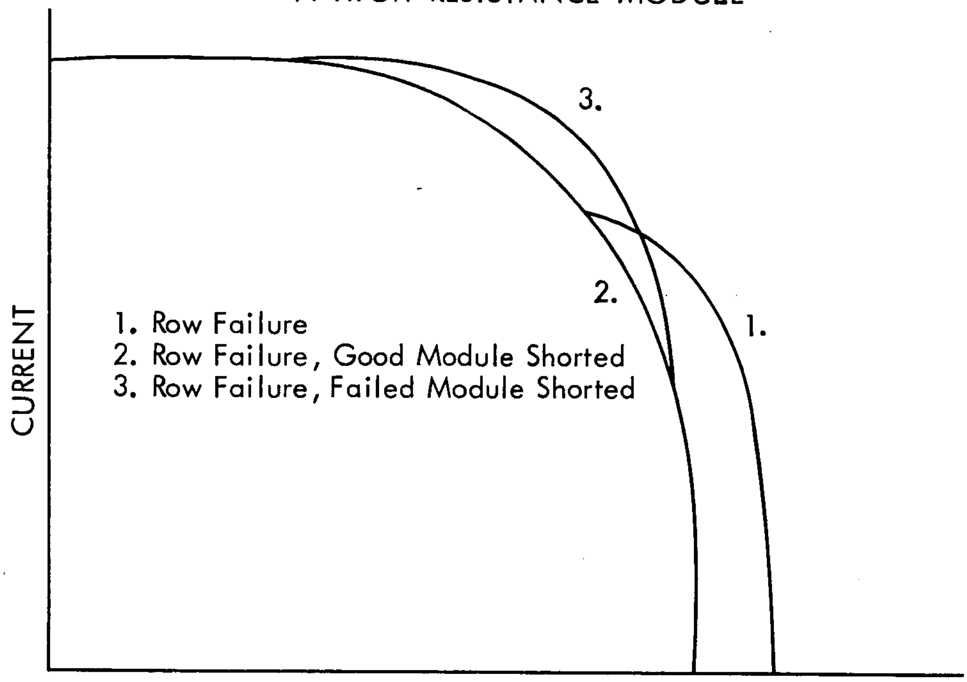


Figure 8

TYPICAL I-V CHARACTERISTICS OF NORMAL AND DEGRADED PATCH

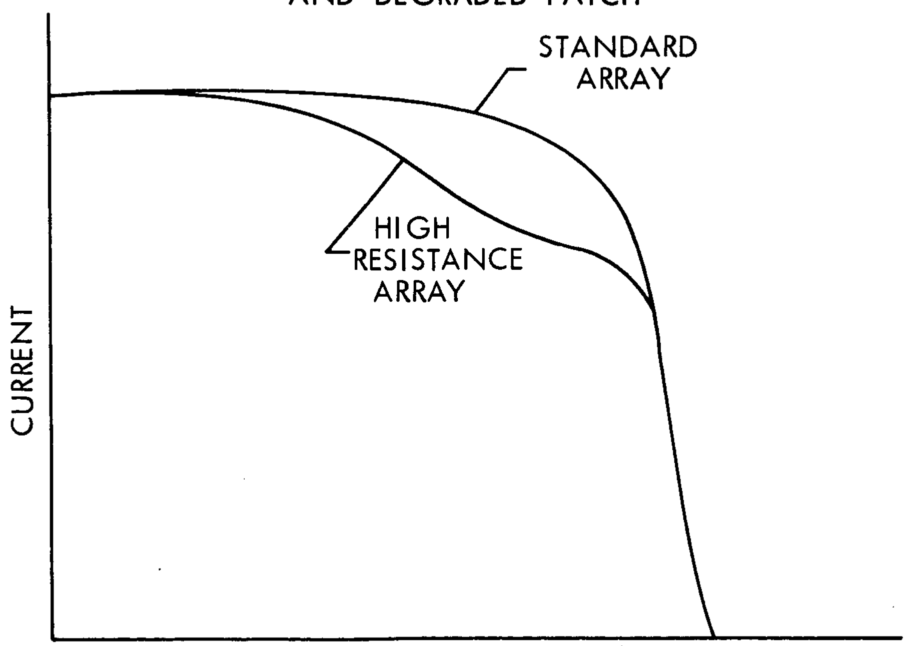


Figure 9

Once the faulty module is isolated, it is unsoldered from the array and a high current, 25-amps, forced through each cell. The RTV heats and the cells can be lifted and removed. The area is cleaned and replaced with a good module.

Both problems associated with the array program revolved around illumination testing. First, since the array is bonded directly to the satellite substrate, illumination testing was limited to availability of the spacecraft from the assembly and integration areas. Secondly, since a given patch is spread over a relatively large area of a curved surface, the normal illumination varies over the patch. The patch output is thereby limited because some of the modules within the patch are more inclined from the normal incidence than others, thus given lower output. Therefore, it is desirable to restrict the size of the patches so that the illumination variance over them is minimized. Therefore, future designs should consider the use of 1 x 2 cm cells mounted on flat detachable substrates to enhance access for test and calibration and to decrease the variance of illumination within a patch. The detachable feature would also enable storage of the array through the months of the program when it is not needed.